is described by the mean anomaly l or equivalently the mean longitude $\lambda \equiv l + \omega$. Collectively these variables are called orbital elements. In the Kepler problem, where a single planet orbits a spherical star, all the elements of the planet except the mean longitude are fixed, which is why the elements are useful quantities. We use the masses and a, e, and i from the JPL ephemeris DE200 (Table 2).
6. B. V. Chirikov, *Phys. Rep.* **52**, 263 (1979); A. J. Lichtenberg and M. A. Lieberman, *Regular and Chaotic Dynamics* (Springer-Verlag, New York, 1992).
7. M. Holman and N. Murray, *Astron. J.* **112**, 1278 (1996).
8. B. Peirce, *ibid.* **1**, 1 (1849); U.-J. Le Verrier, *Annales de L'Observ. Imp. de Paris* **1**, 1 (1855); a modern computer algebraic expansion to eighth order is given by C. D. Murray and D. Harper, *Expansion of the Planetary Disturbing Function to Eighth Order in the Individual Orbital Elements* (QMW Maths Notes, School of Mathematical Sciences, London, 1993).
9. F. Moulton, *An Introduction to Celestial Mechanics* (Dover, New York, 1970), p. 361.
10. N. Murray and M. Holman, *Astron. J.* **114**, 1246 (1997).
11. ———, M. Potter, *ibid.* **116**, 2583 (1998); A. Morbidelli and D. Nesvorney, *ibid.*, p. 3029; for example, our integrations of asteroid 7690 Sackler show that it is in a three-body resonance involving the asteroid, Jupiter, and Saturn.
12. J. Wisdom and M. Holman, *Astron. J.* **102**, 1528 (1991).
13. M. Standish, personal communication.
14. J. Wisdom, M. Holman, J. Touma, *Fields Inst. Commun.* **10**, 217 (1996).
15. A similar survey is reported by G. D. Quinlan, in *IAU Symposium 152* (Kluwer, Dordrecht, Netherlands, 1992).
16. See, for example, S. V. W. Beckwith, A. Sargent, R. S. Chini, R. Guesten, *Astron. J.* **99**, 924 (1990); K. R. Stapelfeldt *et al.*, *Astrophys. J.* **502**, L65 (1998); A. Dutrey *et al.*, *Astron. Astrophys.* **338**, L63 (1998).
17. P. Goldreich and S. Tremaine, *Astrophys. J.* **241**, 425 (1980).
18. J. A. Fernandez and W.-H. Ip, *Icarus* **58**, 109 (1984); R. Malhotra, *Nature* **365**, 819 (1993); *Astron. J.* **110**, 420 (1995); N. Murray, B. Hansen, M. Holman, S. Tremaine, *Science* **279**, 69 (1998).
19. M. Mayor and D. Queloz, *Nature* **378**, 355 (1995); D. W. Latham, R. P. Stefanik, T. Mazeh, M. Mayor, G. Burki, *ibid.* **339**, 38 (1989); G. W. Marcy and R. P. Butler, *Astrophys. J.* **464**, L147 (1996); R. P. Butler, G. W. Marcy, E. Williams, H. Hauser, P. Shirts, *ibid.* **474**, L115 (1997); R. W. Noyes *et al.*, *ibid.* **483**, L111 (1997); *ibid.* **487**, L195 (1997).
20. We thank B. Gladman and J. Wisdom for helpful conversations. Supported by NSERC of Canada.

28 September 1998; accepted 8 February 1999

REPORTS

Compositional Stratification in the Deep Mantle

Louise H. Kellogg,[1]* Bradford H. Hager,[2] Rob D. van der Hilst[2]

A boundary between compositionally distinct regions at a depth of about 1600 kilometers may explain the seismological observations pertaining to Earth's lower mantle, produce the isotopic signatures of mid-ocean ridge basalts and oceanic island basalts, and reconcile the discrepancy between the observed heat flux and the heat production of the mid-ocean ridge basalt source region. Numerical models of thermochemical convection imply that a layer of material that is intrinsically about 4 percent more dense than the overlying mantle is dynamically stable. Because the deep layer is hot, its net density is only slightly greater than adiabatic and its surface develops substantial topography.

Several fundamental constraints must be satisfied by a successful model of the dynamics and thermochemical structure of Earth's mantle. The model must produce sufficient heat, either by radioactive decay or by cooling of the planet, to account for the inferred global heat flux. The model must be capable of producing the rich variety and the observed systematics of geochemical signatures in mantle-derived basalts (*1*). The model must be consistent with inferences from seismic tomography that some subducted slabs extend to near the base of the mantle (*2*) and that the lowermost mantle is characterized by long wavelength structure (*3, 4*) and complex relations between the bulk sound and shear wavespeed (*5, 6*) [see (*7*) for an overview]. Finally, the model must be dynamically consistent. Here, we present a model that is dynamically feasible and satisfies the essential geochemical and geophysical observations. It differs from many previous models by placing a boundary between compositionally distinct mantle regions deep in the lower mantle, rather than at a depth of 660 km.

The characteristic isotopic ratios of mid-ocean ridge basalts (MORB) and oceanic island basalts (OIB) provide evidence for a suite of distinct reservoirs in the mantle (*1*). These reservoirs and signatures are thought to be produced by the formation and recycling of oceanic crust and lithosphere, plus small amounts of recycled continental crust. In addition, ^{129}Xe, $^{3}He/^{4}He$, and ^{40}Ar contents of the mantle (*8–10*) indicate that the mantle has not been entirely outgassed.

$^{87}Sr/^{86}Sr$ and $^{143}Nd/^{144}Nd$ isotope ratios of the crust and MORB have been used to estimate the mass of mantle from which the crust was extracted, and hence to infer the mass of the remaining, less depleted component. Estimates for the mass of the depleted mantle range from 25% (*11*) (coincidentally the mass of the mantle above the 660-km discontinuity) to 90% (*1*). Similar mass balance arguments are used to determine the amount of mantle that must have been outgassed to produce the ^{40}Ar in Earth's atmosphere (*10*); these predict a volume of degassed mantle of ~50%. Uncertainties arise because the K/U ratio of Earth is still under debate (*12*) and the lower crust or the undegassed parts of the mantle have retained substantial amounts of ^{40}Ar (*13*), or some Ar may be recycled.

Another fundamental constraint is provided by Earth's heat budget (*14, 15*). Of the 44 TW (*16*) of the present-day heat flux out of Earth, 6 TW is generated within the crust by radioactive decay of U, Th, and K, and 38 TW must be provided either by generation of heat within the mantle and core or by cooling of the planet (*17*). For example, if Earth had the radiogenic heat production of the average chondritic meteorite, the total heat production would be 31 TW; the remaining 13 TW would be provided by cooling of the planet by 65 K per 10^9 years. Geochemical analyses of basalts, however, show that the source region of MORBs is depleted in heat production by a factor of 5 to 10 relative to a chondritic silicate value (*18*). Thus, if the MORB source region made up most of the mantle, the mantle heat production would be only 2 to 6 TW, comparable to that of the crust. Matching the observed heat flux would require rapid cooling of the planet by, on average, 175 K per 10^9 years, which requires excessive internal temperatures during the Archaean (*19*).

Hence, there must be an extra heat source. The D'' region, a layer of anomalous seismic velocities several hundred kilometers thick at the base of the lower mantle, is likely to be compositionally distinct (*20*), but it can account for only a small fraction of the global heat flux unless there is extreme internal heat production. The latter is unlikely, in particular if the D'' layer contains foundered oceanic crust (*21*), which has a heat production comparable to that of the chondritic silicate Earth (*17*), or some core material (*22*), which is likely low in U, Th, and K.

The energy calculations and geochemical mass balances both suggest that the mantle is composed of several reservoirs: a depleted region, which is the source of MORB; a region that, relative to the MORB source, is unde-

[1]Department of Geology, University of California, Davis, CA 95616, USA. [2]Department of Earth, Atmospheric, and Planetary Sciences, Massachusetts Institute of Technology, Cambridge, MA 01239, USA.

*To whom correspondence should be addressed.

pleted in incompatible elements; and smaller volumes containing fragments of subducted lithosphere (including crust). Because mid-ocean ridges sample the shallow mantle over a wide area of the surface and have relatively uniform composition, it is generally assumed that the upper mantle is depleted. As a consequence, a wide range of models have been based on the assumption that the undepleted reservoir corresponds to the lower mantle (*1*) but that some plumes rise through this region (*23*) or originate at its lower boundary (*1, 24*). Models involving layering of convective flow with a boundary at 660 km are, however, at odds with the seismological evidence (*2*).

We propose instead that the transition in seismological heterogeneity observed at ~1600 km depth (*7*) is the manifestation of a boundary between the depleted MORB source region and enriched, intrinsically dense material in the deeper mantle (Fig. 1). A compositionally distinct layer in the deep mantle would provide an explanation for long-lived geochemical reservoirs; with about 20 to 30% of the mantle volume, it is sufficiently massive to contain the ^{40}Ar and ^{3}He that have not been lost to the atmosphere. In the transition zone above the dense layer, recycled subducted material, mixed with depleted and enriched mantle, would form the complex family of geochemical components seen in oceanic basalts. In this model, the deep, dense layer provides the missing heat production needed to explain the observed heat flux. Such a layer could develop during the early differentiation of Earth, by processes associated with a deep magma ocean, or by formation and recycling of a mafic crust in the Archaean (*25*).

To determine whether this model is dynamically plausible, we used a finite-element model of mantle convection (*26*) modified for thermochemical convection (*27*) to examine the interaction of a subducting slab with an intrinsically dense layer in the deep mantle. Viscosity is temperature- and pressure-dependent (*28*), and plate-like behavior is induced in the cold surface boundary layer by providing weak zones at the upper corners of the box (*29*). An isothermal boundary condition at the core-mantle boundary (CMB) heats the mantle from below at a Rayleigh number of 2×10^7 (*30*). The mantle is also heated from within; in the upper layer, the internal heating Rayleigh number is $Ra_h = 1.16 \times 10^8$ [corresponding to a U concentration of 7 ppb with Th/U = 2.5 and K/U = 10^4 (*18, 31*)]. The deep layer is enriched in heat-producing elements with $Ra_h = 5.12 \times 10^8$, corresponding to a U concentration of 25.6 ppm with Th/U = 4.

Figure 2 shows a snapshot of the resulting temperature and composition (Fig. 2A) and viscosity (Fig. 2B) for the mantle after a subducting slab has penetrated the intrinsically dense layer (*32*). In this simulation—for which we used a buoyancy number $B = \Delta\rho_C/\rho_0\alpha_T\Delta T = 0.9$ (corresponding to an intrinsic density contrast of ~4%), where $\Delta\rho_C$ is density change due to composition alone, ρ_0 is the reference density, α_T is the coefficient of thermal expansion, and ΔT is the temperature drop across the mantle—the dense layer is stable for the duration of the calculation. Because $B < 1$, this model is in the regime of penetrative convection (*33, 34*). The high-viscosity downwelling slab penetrates to the CMB, and steep, large-amplitude topography develops on the interface (*35*). Because the deep layer contains more heat-producing elements, the heat flow across the CMB is lower than it would need to be if the entire mantle had a heat production corresponding to the MORB source region. In this model, the vertical thermal gradient across the thermal boundary layer at the interface between the two domains is larger than that across the thermal boundary layer at the CMB. The interface contains a mix of depleted and subducted material. Plumes arise from high spots on the boundary and carry a mix of depleted material, plus a small amount of entrained material from the less depleted lower layer (*36*).

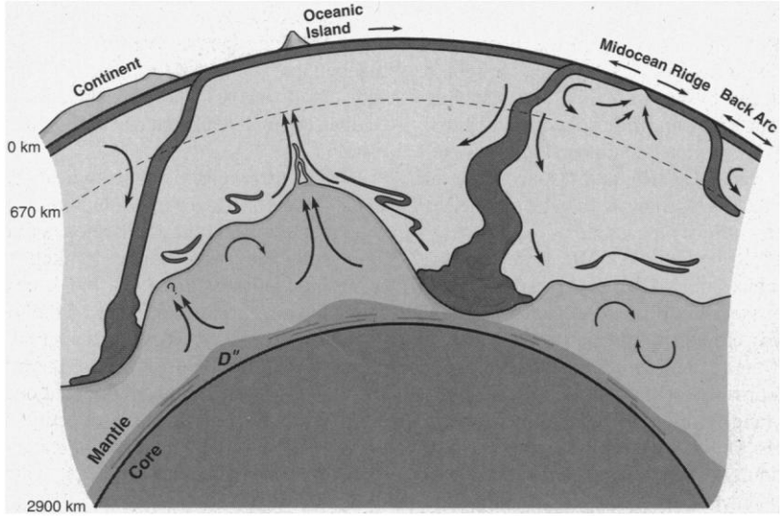

Fig. 1. Diagram illustrating the possible dynamics of an intrinsically dense layer in the lower mantle. Depth to the top of the layer ranges from ~1600 km to near the CMB, where it is deflected by downwelling slabs. Internal circulation within the layer is driven by internal heating and by heat flow across the CMB. A thermal boundary layer develops at the interface, and plumes arise from local high spots, carrying recycled slab and some primordial material.

Because of numerical diffusion, our convection model overestimates the rate at which material in the undepleted layer is entrained by plumes; thus, the rate of entrainment and mixing between layers that we calculate is an upper bound. Even with this small artificial diffusivity, the layers in our calculations remain compositionally distinct for at least 10 overturn times (billions of years). Scaling of mixing rates and dynamic topography with viscosities suggests that mixing was less efficient and the layer more stable in the past (*37*), so a compositionally distinct layer with the intrinsic density contrast that we propose should be stable over the age of Earth.

To quantify the effects of intrinsic density contrasts on the net properties, we compare the average density as a function of depth for these models with that of a reference model with the same viscosity law but with uniform composition. The reference model with uniform composition exhibits a subadiabatic density increase of $\sim 0.1\rho_0\alpha_T\Delta T$ that results from the accumulation of cold material in the lower mantle (Fig. 2D, dashed line). For the compositionally stratified model, assuming a volumetric coefficient of thermal expansion for the lower mantle of $\alpha_T = 2 \times 10^{-5}$ K^{-1} and $\Delta T = 1800$°C, the increase in density due to composition alone (green, Fig. 2D) is ~4%. This density increase is not abrupt but is distributed over the bottom half of the domain in a way that mimics the topography of the boundary between the compositionally distinct layers. There is a nearly compensating decrease in density due to increasing temperature (red, Fig. 2D). For the compositionally layered case (blue, Fig. 2D), the total density excess over that for the uniform composition reference model is never more than ~1%.

When mineral physics estimates of density and seismic velocity as a function of depth for a particular model composition are compared with estimates from analyses of the normal modes of Earth's free oscillation, the results suggest that the lower mantle is ≤2% more dense than would be expected if it were made of the composition estimated for the upper mantle (*38, 39*). This range encompasses the net density increase in our models (Fig. 2C). There are, however, a number of complicating factors. First, although the density averaged

over depths on the order of 1000 km can be determined from normal mode data to an accuracy of better than 0.3% (*40*), there is little resolving power to determine the variations over shorter distances. Earth models typically start from the hypothesis that density variations are adiabatic, but variations of at least 0.5% over a depth range of ~100 km are possible (*41*). Second, mineral physics estimates of density in the lower mantle require knowledge of both the temperature and the thermal expansion coefficient, neither of which is well determined. Third, our convection calculations are for an incompressible model with constant thermal expansivity, which complicates comparisons with Earth. Within these uncertainties, however, our model appears to be consistent with the constraints from seismology and mineral physics.

If a stable, dense layer exists, the amplitude and pattern of *S*- and *P*-velocity anomalies deep in the mantle would depend on whether the increase in density results from enrichment in iron or silicon. To first order, Fe enrichment (Fig. 3A) does not affect the elastic modulus of perovskite, so the main effect is a wavespeed reduction due to increased density (*42*). Changing the Si content alters the relative proportion of perovskite and magnesiowüstite, leading to a lower layer that is seismically fast even though it is hot (Fig. 3B). Thus, adding some Si to an Fe-enriched region would reduce the large velocity variations of Fig. 3A to reasonable values. Both components may be important in Earth.

We do not have precise constraints on the volume of the depleted mantle. The change in seismic signature characterized by the radial correlation function (*7*) and an investigation of possible nonadiabatic density jumps (*41*) suggest that this transition should begin at a depth in excess of 1500 km. The high amplitude of topography on the interface may lead to incoherent scattering and complicate the interpretation of radial correlation functions, which average out signals over a wide lateral region. Because of the dynamic topography, the interface would more likely manifest itself as regional discontinuities of variable depths, locally perhaps as shallow as 1200 km, and the interface might therefore lead to incoherent scattering. Through analysis of scattered waves, seismol-

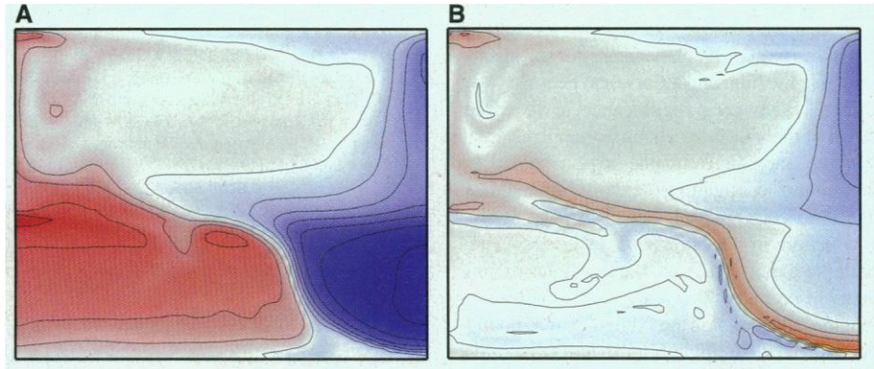

Fig. 3. Model seismic velocities (lateral variations in $\partial V_s/V_s$) assuming that the intrinsic density increase in the lower layer is due to enrichment in (**A**) Fe or (**B**) Si (*39*, *42*). Contour intervals are 1%.

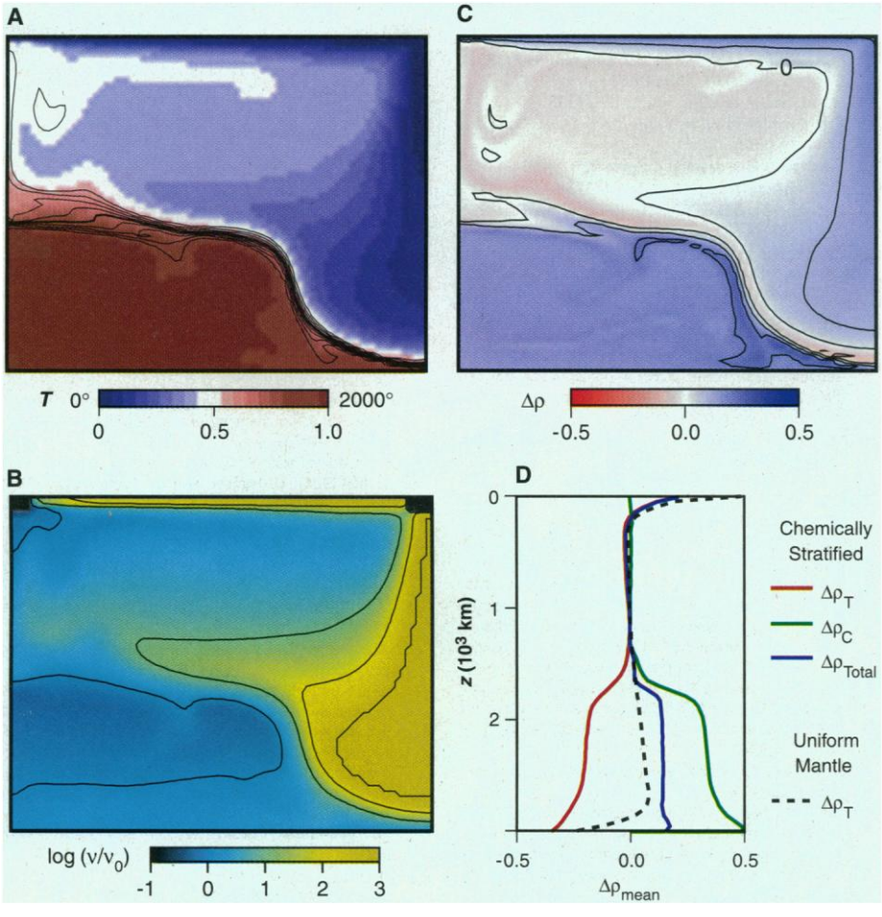

Fig. 2. Numerical simulation of a dense layer, enriched in heat-producing elements, at the base of the mantle. (**A**) Temperature (color) is elevated in the dense layer; a thermal boundary layer is visible on the interface between the two materials. Contours of composition (lines) illustrate large-scale topography on the interface; in this model, with $B = 0.9$, a subducting slab on the right side (blue) nearly reaches the CMB. A small amount of dense material is entrained in the hot plume (white) rising from the peak of the layer. (**B**) The cold slab retains a high viscosity ν (*28*), whereas the higher temperature in the lower layer tends to counteract the effect of pressure on viscosity. (**C**) Density $\Delta\rho$, relative to the mean density at a depth of 1100 km (above the compositional boundary). On this nondimensional scale, ± 0.5 corresponds to ± 2 to 4%. (**D**) Laterally averaged densities for the model in (A) to (C) and for a reference model containing no compositional variations (dashed line) are plotted with respect to their values at a depth of 1100 km. Net density varies by less than 1% compared to the reference model. $\Delta\rho_T$ is density change due to temperature alone, $\Delta\rho_C$ is density change due to composition alone, and $\Delta\rho_{Total}$ is the net density for the chemically stratified model.

ogists may be able to identify the nature and morphology of this feature. Simulations of the substantially thinner D'' layer in two dimensions (*43*) and in three dimensions (*34*) show that compositionally dense material piles up under upwellings [possibly explaining the superplume structures seen under Africa, for example (*34*)] and that some dense material is entrained in upwellings (*34, 36*). These simulations exhibit varying degrees of topography on D'', depending on the density of the layer. Further studies will be required to determine how convection in the relatively thick, dense layer that we propose relates to the D'' region.

Because our calculations are for an incompressible medium and a Cartesian geometry, we cannot assign great significance to the exact depth of the interface. The important concept is that the anomalous mantle region should be voluminous enough to generate substantial heat and is not easily swept out of the way by the convection in the overlying layer associated with plate motions. Also, the dynamics of convection seem to favor massive, long-wavelength deflections of the compositional boundary, rather than highly localized penetrative convection (*44*).

The seismic signature of the downwelling slab is apparent through the upper two-thirds of the mantle. At greater depths, where the slab has encountered the dense layer, the signature of the slab becomes weaker, broader, and more complex. Although it is clear from the temperature and composition that the slab reaches to near the CMB, its seismic signal is diffuse. In Earth, we would expect to see variability along the strike of the slab as well. Models of downwellings in a spherical shell indicate that slab-like structures may be expected to break up into drips in the deep mantle (*45*). Lateral variations in the age of slabs originating from different tectonic settings will also affect the ability of a slab to deflect the boundary. We therefore envision slab penetration to near the CMB as being a relatively rare and probably short-lived event.

Fossil subducted slabs would collect at the interface between the two materials. A thermal boundary layer at the interface would generate plumes that rise to the surface, carrying components of ancient slab as well as sometimes carrying components of the dense layer itself. Plumes would tend to arise from local high spots on the interface; these high spots act to stabilize the location of plumes. Because the surface of the interface varies with depth, plumes could originate at depths ranging from 1600 km to perhaps the CMB.

References and Notes

1. A. W. Hofmann, *Nature* **385**, 219 (1997).
2. R. D. van der Hilst, S. Widiyantoro, E. R. Enghdahl, *ibid.* **386**, 578 (1997).
3. W. J. Su, R. L. Woodward, A. M. Dziewonski, *J. Geophys. Res.* **99**, 6945 (1994).
4. X.-F. Liu and A. M. Dziewonski, in *The Core-Mantle Boundary Region,* M. Gurnis, M. E. Wysession, E. Knittle, B. Buffett, Eds., vol. 28 of *Geodynamics* (American Geophysical Union, Washington, DC, 1998), pp. 21–36.
5. W. J. Su and A. M. Dziewonski, *Phys. Earth Planet. Inter.* **100**, 135 (1997).
6. B. L. N. Kennett, S. Widiyantoro, R. D. van der Hilst, *J. Geophys. Res.* **103**, 12469 (1998).
7. R. D. van der Hilst and K. Kárason, *Science* **283**, 1885 (1999).
8. J. Kunz, T. Staudacher, C. J. Allègre, *ibid.* **280**, 877 (1998).
9. H. Craig and J. E. Lupton, *Earth Planet. Sci. Lett.* **31**, 369 (1976).
10. C. J. Allègre, T. Staudacher, P. Sarda, M. Kurz, *Nature* **303**, 762 (1983); D. L. Turcotte and G. Schubert, *Icarus* **74**, 36 (1988); C. J. Allègre, A. Hofmann, R. K. O'Nions, *Geophys. Res. Lett.* **23**, 3555 (1996).
11. S. B. Jacobsen and G. J. Wasserburg, *J. Geophys. Res.* **84**, 7411 (1979); G. J. Wasserburg and D. J. DePaolo, *Proc. Natl. Acad. Sci. U.S.A.* **76**, 3594 (1979); R. K. O'Nions, N. M. Evensen, P. J. Hamilton, *J. Geophys. Res.* **84**, 6091 (1979).
12. F. Albarède, *Chem. Geol.* **145**, 413 (1998).
13. E. Chamorro-Pérez, P. Gillet, A. Jamon, J. Badro, P. McMillan, *Nature* **303**, 352 (1998).
14. R. K. O'Nions, N. M. Evensen, P. J. Hamilton, S. R. Carter, *Philos. Trans. R. Soc. London Ser. A* **288**, 547 (1978).
15. R. K. O'Nions and E. R. Oxburgh, *Nature* **306**, 429 (1983).
16. C. A. Stein, in *Global Earth Physics: A Handbook of Physical Constants,* T. A. Ahrens, Ed. (American Geophysical Union, Washington, DC, 1995), pp. 144–158.
17. R. J. O'Connell and B. H. Hager, in *Physics of the Earth's Interior*, vol. 78 of *Proceedings of the International School of Physics "Enrico Fermi,"* A. M. Dziewonski and E. Boschi, Eds. (North-Holland, Amsterdam, 1980), pp. 270–317.
18. K. P. Jochum, A. W. Hofmann, E. Ito, H. M. Seufert, W. M. White, *Nature* **306**, 431 (1983).
19. F. M. Richter, *Earth Planet. Sci. Lett.* **73**, 350 (1985); S. Honda, *ibid.* **131**, 357 (1995).
20. M. Wysession *et al.*, in (*4*), pp. 273–297.
21. A. Hofmann and W. M. White, *Earth Planet. Sci. Lett.* **57**, 421 (1982).
22. E. Knittle and R. Jeanloz, *Science* **251**, 1438 (1991).
23. J. G. Schilling, *Nature* **242**, 565 (1973).
24. C. J. Allègre and D. L. Turcotte, *Geophys. Res. Lett.* **12**, 207 (1985).
25. Hf isotopes indicate that the Archaean mantle underwent early depletion [J. D. Vervoort, P. J. Patchett, G. E. Gehrels, A. P. Nutman, *Nature* **379**, 624 (1996)] before 3.6×10^9 to 3.8×10^9 years ago, possibly by extraction of a mafic crust that was then recycled into the mantle (J. D. Vervoort and J. Blichert-Toft, *Geochim. Cosmochim. Acta,* in press). Such recycled mafic crust could be a substantial component of the dense layer we propose here.
26. S. D. King, A. Raefsky, B. H. Hager, *Phys. Earth Planet. Inter.* **59**, 195 (1989).
27. P. E. van Keken *et al.*, *J. Geophys. Res.* **102**, 22477 (1997).
28. We use an Arrhenius form of the viscosity law, $\nu = \nu_0 \exp\{[(E^* + V^*\zeta)/(\theta + \theta_0)] - [(E^* + V^*\zeta_0)/(1.0 + \theta_0)]\}$, where θ is dimensionless temperature ($0 \leq \theta \leq 1$), ζ is dimensionless depth, ν_0 is a "reference" viscosity for $\theta = 1$ and $\zeta = \zeta_0$, and E^* and V^* are the normalized activation energy and activation volume, respectively. We used $E^* = 3$ with $\theta_0 = 0.2$, providing a factor of 1000 contrast in viscosity between the hottest and coldest mantle at constant pressure, and $V^* = 3$, with $\zeta_0 = 0.1$. Weak zones at the upper left and right corners are uniform viscosity of $\nu_{weak} = 0.1\nu_0$.
29. S. D. King, C. W. Gable, S. A. Weinstein, *Geophys. J. Int.* **109**, 481 (1992).
30. The basal heating Rayleigh number is defined using the reference viscosity ν_0: $Ra = \rho_0 g \alpha_T \Delta T d^3 / \nu_0 \kappa$, where g is gravitational acceleration, d is the depth of the mantle, ν_0 is the reference viscosity (*28*), and κ is thermal diffusivity.
31. G. J. Wasserburg, G. J. F. MacDonald, F. Hoyle, W. A. Fowler, *Science* **143**, 65 (1964).
32. Initial conditions of the model were obtained by imposing a barrier to radial flow at 2000 km depth, separating the two reservoirs, and allowing the model to reach a statistical steady state. The resulting temperature was used to determine an initial model geotherm, and a thermal profile for a plate ranging from the present day (left corner) to 4×10^8 years ago (right corner) was introduced using a half-space cooling model. The mid-mantle barrier was then removed.
33. P. Olson, P. G. Silver, R. W. Carlson, *Nature* **344**, 209 (1990).
34. P. J. Tackley, in (*4*), pp. 231–253.
35. Although we have not attempted to determine precisely the minimum intrinsic density contrast for which the dense layer is stable, we explored a wide range of parameters for this model, including $B = 0$ to 1 and a range of enriched and depleted lower layers. The stability of the dense layer depends in part on the rate of heat production in the layer. A model containing a depleted, intrinsically dense layer was stable for intrinsic density contrasts of ~2% because the layer remained relatively cooler; such a depleted layer does not satisfy mantle heat flow constraints, however.
36. N. H. Sleep, *Geophys. J.* **95**, 437 (1988).
37. Entrainment of the dense layer is driven by viscous stresses from convection in the overlying layer. The entrainment rate scales as the product of velocity and viscosity. Boundary layer theory suggests that convective velocity scales as $Ra^{2/3}$. Because of the extreme dependence of mantle viscosity on temperature, Ra scales as ν^{-1}. Thus, the entrainment rate scales as $\nu^{1/3}$. Tackley (*34*) argues that the boundary deflection should scale as $Ra^{-1/3}$, also equivalent to $\nu^{1/3}$. The mantle is now cooling, so temperatures in the past were higher and viscosities were lower, as were entrainment rates and topography on the interface between internal chemical boundaries.
38. R. Jeanloz and E. Knittle, *Philos. Trans. R. Soc. London Ser. A* **328**, 377 (1989); P. G. Silver and C. Bina, *Geophys. Res. Lett.* **20**, 1135 (1993); I. Jackson, *Geophys. J. Int.* **134**, 291 (1998).
39. Y. Wang, D. J. Weidner, R. C. Liebermann, Y. Zhao, *Phys. Earth Planet. Inter.* **83**, 13 (1994).
40. F. Gilbert, A. Dziewonski, J. Brune, *Proc. Natl. Acad. Sci. U.S.A.* **70**, 1410 (1973).
41. B. L. N. Kennett, *Geophys. J. Int.* **132**, 374 (1998).
42. We determined the shear wave velocity characteristics for Fe enrichment using $\partial V_s/V_s = 1/2\{(1/\rho V_s^2)(\partial\mu/\partial T)\delta T - [\partial(\ln \rho)/\partial T]\delta T - [\partial(\ln \rho)/\partial C]\delta C\}$, where C is composition. We took $\partial\mu/\partial T = -2 \times 10^7$ Pa/K (*46*), $\alpha_T = 2 \times 10^{-5}$ K^{-1}, and scaled the nondimensional temperature of the model to 1800 K. Hence, if the increased intrinsic density of the lower layer is assumed to be due to enrichment in Fe, the model composition and temperature give $\partial V_s/V_s = -8 \times 10^{-2}\Delta\theta - 2 \times 10^{-2}\Delta C$. For Si enrichment, we included the effects of changing composition on changing phase (*46*), obtaining $\partial V_s/V_s = -8 \times 10^{-2}\Delta\theta + 6 \times 10^{-2}\Delta C$.
43. G. F. Davies and M. Gurnis, *Geophys. Res. Lett.* **13**, 1517 (1986); U. Hansen and D. Yuen, *Nature* **334**, 237 (1988); *Geophys. Res. Lett.* **16**, 629 (1989); L. H. Kellogg and S. D. King, *ibid.* **20**, 379 (1993); L. H. Kellogg, *ibid.* **24**, 2749 (1997).
44. P. G. Silver, R. W. Carlson, P. Olson, *Annu. Rev. Earth Planet. Sci.* **16**, 477 (1988).
45. G. A. Glatzmaier, G. Schubert, D. Bercovici, *Nature* **347**, 274 (1990).
46. Y. Wang and D. J. Weidner, *Pure Appl. Geophys.* **146**, 533 (1996).

47. We thank the participants in the MIT-Harvard joint seminar in Mantle Convection, and A. Hofmann for a helpful review of the manuscript. L.H.K. thanks MIT for hosting her visit during which this model was developed, and E. Garnero, B. Romanowicz, and J. Vervoort for stimulating discussions. Supported by an NSF Presidential Faculty Fellowship (L.H.K.) and by NSF grants EAR-9506427 (B.H.H.) and EAR96-28087 (R.D.v.d.H.).

10 November 1998; accepted 3 February 1999